Analysis of the railway track as a spatially periodic structure

J García-Palacios*, **A Samartín,** and **M Melis**

Abstract: This article presents a new and computationally efficient method of analysis of a railway track modelled as a continuous beam of $2N$ spans supported by elastic vertical springs. The main feature of this method is its important reduction in computational effort with respect to standard matrix methods of structural analysis. In this article, the whole structure is considered to be a repetition of a single one. The analysis presented is applied to a simple railway track model, i.e. to a repetitive beam supported on vertical springs (sleepers). The proposed method of analysis is based on the general theory of spatially periodic structures. The main feature of this theory is the possibility to apply Discrete Fourier Transform (DFT) in order to reduce a large system of $q(2N+1)$ linear stiffness equilibrium equations to a set of $2N+1$ uncoupled systems of q equations each. In this way, a dramatic reduction of the computational effort of solving the large system of equations is achieved. This fact is particularly important in the analysis of railway track structures, in which N is a very large number (around several thousands), and $q=2$, the vertical displacement and rotation, is very small. The proposed method allows us to easily obtain the exact solution given by Samartín [**1**], i.e. the continuous beam railway track response. The comparison between the proposed method and other methods of analysis of railway tracks, such as Lorente de Nó and Zimmermann-Timoshenko, clearly shows the accuracy of the obtained results for the proposed method, even for low values of N. In addition, identical results between the proposed and the Lorente methods have been found, although the proposed method seems to be of simpler application and computationally more efficient than the Lorente one. Small but significative differences occur between these two methods and the one developed by Zimmermann-Timoshenko. This article also presents a detailed sensitivity analysis of the vertical displacement of the sleepers. Although standard matrix methods of structural analysis can handle this railway model, one of the objectives of this article is to show the efficiency of DFT method with respect to standard matrix structural analysis. A comparative analysis between standard matrix structural analysis and the proposed method (DFT), in terms of computational time, input, output and also software programming, will be carried out. Finally, a URL link to a MatLab computer program list, based on the proposed method, is given

Keywords: railway track analysis, periodic structures

1 INTRODUCTION

The analysis of repetitive structures, also known in the technical literature, as 'periodic structures' has been greatly simplified using the property of periodicity. In general, periodic structures are analysed by numerical methods without taking advantage of its periodicity property, i.e. the potential computation reduction involved in this type of structures. Usually, matrix structural analysis is applied. Moreover, general analytical solutions cannot be obtained using only numerical approaches. For this reason, several methods that take into account the periodicity property have been developed. A simple class of periodic structures is the so-called rotationally periodic structures, that is described in the pioneer publication [**2**]. Their dynamic behaviour has been studied in the publication [**3**] and extended to infinite spatially periodic structures by Cai et al. [**4**], using a method, equivalent to the one presented by Thomas, called U-transform. The static analysis of spatially periodic structures has been studied by Cheung et al. [**5**] applying the ideas of U-transform. In this article, a general approach to the analysis of rotationally and spatially periodic structures of finite length is applied. In this approach, all the governing equations for all substructures, say N substructures, become N governing uncoupled equations. It is assumed that N is a finite number. The main feature of this approach is the use of discrete Fourier transform (DFT) and its extension to other structures (distinct to the 1D structures, i.e. continuous beams) is straightforward. There exist other procedures to handle periodic problems. In the case of total infinite span, the structural analysis of a spatially periodic structure is described by a continuum, i.e. by an ordinary differential equation with periodic coefficients. In this case, the possibility to apply the modern theory of Floquet transform should be envisaged [**6**, **7**].

Floquet theory is the mathematical theory of linear, periodic systems of ordinary differential equations (ODEs) and as such appears in standard book on ODEs, e.g. Ordinary Differential Equations, by Amann [**8**] on Hale [**9**]. However, the application of Floquet theory to railway tracks with a finite number of sleepers presents some difficulties because, in this case, the mathematical problem to be solved corresponds to a matrix convolution equation. Then, the authors think the DFT perhaps can be more suitable than the Floquet transform in order to solve the problem spatially periodic structures with a finite number or repetitive structures. In this respect, a short discussion is introduced in the paper and references [**6**, **7**], in which Floquet transformations are applied and described.

From a structural point of view, a railway track can be approximated as an infinite continuous beam of very high stiffness (the rail) supported by equidistant elastic supports. This applies both to the so-called slab track as well as to the common ballasted track. However, it does not apply to other types of tracks, where the rail is supported by a continuous elastomeric layer below the rail foot.

The vertical flexibility of the rail supports k^{-1} is the sum of the flexibilities k_i^{-1}, where $i = 1, 2, 3, 4$ corresponds to the pad under the rail, the ballast layer under the sleeper, the subballast layer below and the stiffness of the platform, respectively. Table 1 shows typical values for a ballasted track. In this case, the vertical global stiffness under rail is obtained by the expression:

$$k = \frac{1}{\sum_{i=1}^{4} \frac{1}{k_i}} = 32.0 \text{ kN/mm}$$

This global vertical stiffness of the elements under the rail foot is different from the global vertical stiffness of the track, which includes the flexural stiffness of the rail itself. When a load of 90 kN of the train wheel is located over a sleeper, the rail has a settlement of 1 mm. In this case, the global vertical track stiffness is 90 kN/mm. However, the load that the rail foot transmits to the pad and to the sleeper below is only some part of the total wheel load, because the rest is absorbed by the rail itself. With the method described in this article, this load can be easily calculated. Suppose the result for a certain stiffness of the track under the rail is 32 kN, then the vertical stiffness of the track without the rail is 32 kN/mm compared to 90 kN/mm, taking into account the rail.

In the slab track, there is no ballast and the rails are supported by a concrete slab that can be considered of very high stiffness, which rests on the earthworks. All the flexibility that the track needs is provided by the fastening system. In some slab track for HSL, the fastening system, called IOARV-300, has two pads, one with a stiffness around 450 kN/mm and another one below 22.5 kN/mm. This type of track will have a global vertical stiffness under rail foot of 21.43 kN/mm.

Table 1 Vertical stiffness (kN/mm) for Ballasted track

Material	Stiffness
Pad	100
Ballast	250
Subballast	200
Earthworks	82
Global	32

According to Esveld [10] and Melis [11], there are two main models for the static track design, the continuous or Winkler support model and the discrete rail support. The Winkler model was formulated in 1867 and this model hypothesis is a material constitutive equation, namely, the foundation subsidence u under the load is proportional to the local compressive stress σ, i.e. $\sigma = Cu$, where C is the so-called foundation modulus or ballast modulus, measured in N/m^3, like a specific weight. This model is also known as Zimmermann–Timoshenko model.

In the discrete support model, the track is studied as an infinite continuous beam of very high stiffness, supported by infinite equidistant independent elastic supports of the same stiffness. This stiffness can be known either by calculation or alternatively, it can be obtained using the method presented in this article, which measures the deflexion of the rail under the wheel load acting at a known position.

2 WINKLER OR ZIMMERMANN–TIMOSHENKO MODEL

The above constitutive equation for this simple Zimmermann–Timoshenko model, $\sigma = Cu$, can be integrated easily for the case of a semi-infinite beam of width b. In this case, the ballast reaction force, per unit of length at section x, for a beam deflection $v(x)$, is given by the expression $p(x) = Cbv(x)$. The beam is subjected to a vertical downwards load P_0, acting at section $x = 0$, where due to symmetry the rotation of this section is zero (Fig. 1). The problem is described mathematically [12], by the boundary value problem given by the following equations, in which the beam self-weight is neglected

$$EI\frac{d^4v}{dx^4} + Cbv = 0 \quad \text{at} \quad x \in 0 \le x \le \infty \tag{2.1}$$

$$\frac{dv}{dx} = 0, \quad EI\frac{d^3v}{dx^3} = \frac{P_0}{2} \quad \text{at} \quad x = 0 \tag{2.2}$$

$$v = 0, \quad \frac{dv}{dx} = 0 \quad \text{at} \quad x = \infty \tag{2.3}$$

where $v = v(x)$ is the deflection of the beam at any point x, E the Young modulus, and I the moment of inertia of the beam cross-section.

The solutions to this boundary value problem, given by equations (2.1) to (2.3) are

$$v(x) = -\frac{P_0}{8EI\lambda^3}e^{-\lambda x}(\cos\lambda x + \sin\lambda x),$$
$$\theta(x) = \frac{P_0}{4EI\lambda^2}e^{-\lambda x}\sin\lambda x \tag{2.4}$$

$$M(x) = \frac{P_0}{4\lambda}e^{-\lambda x}(\cos\lambda x - \sin\lambda x),$$
$$Q(x) = -\frac{P_0}{2}e^{-\lambda x}\cos\lambda x \tag{2.5}$$

where $v(x)$, $\theta(x)$, $M(x)$, and $Q(x)$ are the deflection, rotation, bending moment, and shear force at the beam section x, respectively. Finally, λ is a dimensionless constant, describing the soil–structure interaction, which is the defined by the following expression

$$\lambda = \left[\frac{Cb}{4EI}\right]^{\frac{1}{4}}$$

3 MODEL OF A CONTINUOUS BEAM ON DISCRETE EQUIDISTANT ELASTIC SUPPORTS

The Zimmermann–Timoshenko or Winkler model can be refined introducing the equidistant elastic supports which simulate the sleepers. In this model, the beam of cross-section stiffness, EI, is supported by a high number of identical supports. As shown in Fig. 2, each of the vertical stiffnesses, k, is measured in N/m or kN/mm. The mass of the beam is negligible in comparison to the mass of the train wheel. This type of structure was solved by Unold [13] and Dischinger [14] adapted for the track and improved by Lorente de Nó [15]. The latter uses classical structural methods of compatibility in the continuous beam structure, which are solved as recurrence equations. In other earlier railway texts simpler classical methods have been used, such as the Clapeyron method. Finally, other methods are based either on

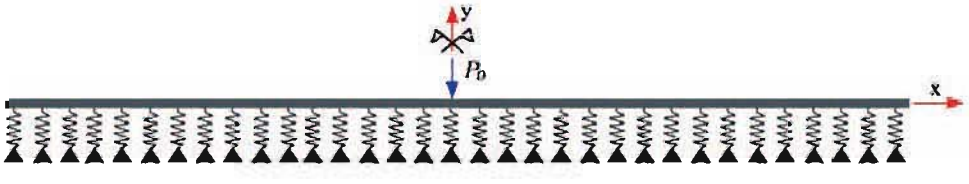

Fig. 1 Winkler or Zimmermann–Timoshenko model

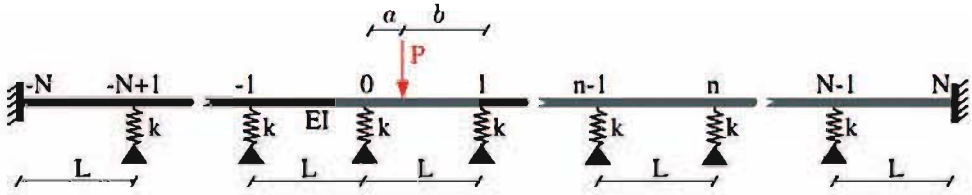

Fig. 2 General load case

the transfer matrix methods, see Livesley [**16**] or on any of the methods used in matrix structural analysis, such as the stiffness or the compatibility methods. The Lorente de Nó recursive method and its railway track applications are described in detail in Lorente de Nó [**15**].

Obviously, there exist more realistic models of the railway behaviour than the static one presented here. One of them is the dynamic model in which inertia forces are included. Additionally, this more realistic model should include the influence of the underneath structures and embankments under the railway tracks. This sophisticated model can also be handled with the DFT technique, assuming a Finite Element model for the underneath structures and embankments. It can be shown that the comparative efficiency of the proposed method could be improved with respect to the standard matrix structural analysis, if underneath structures are modelled together with the railway. However, a more simple model than the former one can be used instead, namely, the simple model of a continuous beam on discrete equidistant elastic supports but with elastic supports of different vertical stiffness between railway sections. These support differences are due to unequal underneath conditions. As will be shown below in one example, in this case, it is still possible to apply a natural extension of the DFT method. Finally, it should be pointed out that dynamic analysis of a continuous beam structure subjected to a mobile train loading has been treated in the technical literature of repetitive structures [**2**, **4**]. However, due to the complexity of the non-linearities involved in the case of railway track analysis its treatment is beyond the scope of this article. If the large mass of the train is also included in the analysis, the total mass of the structure varies with time.

The application of the Theory of Spatially Periodic Structures published in Samartín [**1**] and more recently in Karpov [**17**] gives directly results of displacement and rotation of the rail for each of the N supports, with an efficient computational numerical method, that considers both the obtained accuracy and the computation time.

Being v_n and θ_n the vertical deflection and the rotation of the beam in each n of the N supports, the following vectors are defined, where the variables are dimensionless.

1. State vector

$$\text{Forces} \quad \mathbf{p}_n = \begin{bmatrix} \bar{q}_n \\ \bar{m}_n \end{bmatrix} \text{where} \quad \bar{q}_n = \frac{q_n L^2}{EI}, \quad \bar{m}_n = \frac{m_n L}{EI} \tag{3.1}$$

with q_n the vertical force and m_n the moment acting at support n.

$$\text{Displacements} \quad \mathbf{u}_n = \begin{bmatrix} \bar{v}_n \\ \bar{\theta}_n \end{bmatrix} \text{where} \quad \bar{v}_n = \frac{v_n}{L}, \quad \bar{\theta}_n = \theta_n \tag{3.2}$$

with v_n the vertical displacement and θ_n the rotation produced at the support n.

The index of the generic support n varies from support $-N$ to support N, i.e. the $2N+1$ supports are numbered as follows: $n=-N, -N+1, \ldots, -1, 0, 1, \ldots, N-1, N$

Forces are positive when ascending and rotations are positive if counterclockwise.

2. Constitutive relationship for a beam n, joining nodes (supports) $n-1$ and n, is given by the expressions

$$\begin{bmatrix} \mathbf{p}_{n-1} \\ \mathbf{p}_n \end{bmatrix} = \begin{bmatrix} \mathbf{k}_{11} & \mathbf{k}_{12} \\ \mathbf{k}_{12} & \mathbf{k}_{22} \end{bmatrix} \begin{bmatrix} \mathbf{u}_{n-1} \\ \mathbf{u}_n \end{bmatrix} + \begin{bmatrix} \mathbf{p}^0_{n-1} \\ \mathbf{p}^0_n \end{bmatrix} \tag{3.3}$$

with $\mathbf{k}=[\mathbf{k}_{ij}]$ $(i, j=1, 2)$, the stiffness matrix of the beam and, $-\mathbf{p}^0_{n-1}$ and $-\mathbf{p}^0_n$ the fixed-end force vectors at beam nodes $n-1$ and n, due to eventual loading acting directly at the span of the beam.

Therefore, the stiffness submatrices relating the former dimensionless variables are given in Livesley [**16**]

$$\mathbf{k}_{11} = \begin{bmatrix} 12+0.5\bar{k} & 6 \\ 6 & 4 \end{bmatrix}, \mathbf{k}_{12} = \begin{bmatrix} -12 & 6 \\ -6 & 2 \end{bmatrix}, \quad \mathbf{k}_{22} = \begin{bmatrix} 12+0.5\bar{k} & -6 \\ -6 & 4 \end{bmatrix} \tag{3.4}$$

where $\mathbf{k}_{21} = \mathbf{k}^T_{12}$, and $\mathbf{p}$ and $\mathbf{u}$ are the force and displacement vectors, respectively, at the element n, $(n=-N, -N+1, \ldots, N-1, N)$. The dimensionless

variable $\bar{k} = kL^3/EI$ corresponds to the stiffness with k being the actual stiffness of the beam supports.

4 ANALYSIS OF THE TRACK AS A PERIODIC STRUCTURE

The application of the concepts of circulant matrices and the DFT to the cyclic and spatially periodic structures has been reported in the scientific literature by several authors, see for example the early work by Samartín [1] and the interesting publication by Karpov [17]. This article will show the efficiency of this methodology in the study of the displacement and stress analysis produced in a railway track under the wheel load.

The general case of a beam with $2N$ spans, where a set of p_n loads $n=-N$, $(N-1)$,..., $N-1$, N acting on the supports is considered first. The case where the wheel is placed between the two supports of span number 1, at distances a and b of supports 0 and 1, so that $a+b=L$, is studied next. The distances will be considered in this dimensionless form $\bar{a}=\frac{a}{L}$ and $\bar{b}=\frac{b}{L}$, so that $\bar{a}+\bar{b}=1$. In this case, the concentrated wheel load P, downwards negative, is acting between supports 0 and 1, and the reactions, as a fixed-end beam are written in dimensionless form as follows:

$$\begin{bmatrix} \mathbf{p}_0^0 \\ \mathbf{p}_1^0 \end{bmatrix} \quad \text{with} \quad \mathbf{p}_n^0 = \begin{bmatrix} \bar{q}_n^0 \\ \bar{m}_n^0 \end{bmatrix}, \quad (n=0,1) \tag{4.1}$$

where

$$\begin{aligned} &\bar{q}_0^0 = -\bar{P}(1+2\bar{a})\bar{b}^2,\ \bar{m}_0^0 = -\bar{P}\bar{a}\bar{b}^2, \\ &\bar{q}_1^0 = -\bar{P}(1+2\bar{b})\bar{a}^2,\ \bar{m}_1^0 = \bar{P}\bar{b}\bar{a}^2 \end{aligned} \tag{4.2}$$

and $\bar{P}=\frac{PL^2}{EI}$ the dimensionless expression of the acting load, negative downwards.

The complete structure with $2N$ spans is considered and the force $\bar{P}$ is replaced by the equivalent forces $\mathbf{p}_0=-\mathbf{p}_0^0$ and $\mathbf{p}_1=-\mathbf{p}_1^0$ at supports 0 and 1. These equivalent forces produce the same effect than the load $\bar{P}$ acting on span 0-1. Reactions on the other supports are null, i.e. $\mathbf{p}_n=0$ for $n=-1$, ±2, ±3,..., $\pm(N-1)$. If the number of spans $2N$ is high the extreme supports $-N$ and N can be considered as fixed,* and then $\mathbf{u}_{-N}=0$ and $\mathbf{u}_N=0$. If these two nodes are fixed-end supports, it implies there are reactions $\mathbf{r}_{-N}$ and $\mathbf{r}_N$ which have to be calculated, and there exist, accordingly the actions $\mathbf{p}_{-N}=\mathbf{r}_{-N}$ and $\mathbf{p}_N=\mathbf{r}_N$ at these two nodes. In addition, it is possible to consider the complete cyclic structure with period $2N+1$, i.e. $\mathbf{u}_{-N}=\mathbf{u}_N$. The equilibrium equations at each of the nodes n are written as follows

$$\mathbf{k}_{11}\mathbf{u}_{-N} + \mathbf{k}_{12}\mathbf{u}_{-N+1} = \mathbf{r}_{-N}, \quad n=-N \tag{4.3}$$

$$\begin{aligned} &\mathbf{k}_{21}\mathbf{u}_{n-1} + (\mathbf{k}_{22}+\mathbf{k}_{11})\mathbf{u}_n + \mathbf{k}_{12}\mathbf{u}_{n+1} = \mathbf{p}_n, \\ &\quad n=0,\ \pm1,\ldots,\ \pm(N-1) \end{aligned} \tag{4.4}$$

$$\mathbf{k}_{21}\mathbf{u}_{N-1} + \mathbf{k}_{22}\mathbf{u}_N = \mathbf{r}_N, \quad n=N \tag{4.5}$$

Defining $\mathbf{k}_1=\mathbf{k}_{21}$, $\mathbf{k}_0=\mathbf{k}_{22}+\mathbf{k}_{11}$, and $\mathbf{k}_{-1}=\mathbf{k}_{12}$, this system of equations can be rewritten as

$$\begin{aligned} &\mathbf{k}_1\mathbf{u}_{n-1} + \mathbf{k}_0\mathbf{u}_n + \mathbf{k}_{-1}\mathbf{u}_{n+1} = \mathbf{p}_n^* \\ &\quad n=0,\ \pm1,\ \pm2,\ldots,\ \pm N \end{aligned} \tag{4.6}$$

where the loads are defined as follows

$$\begin{aligned} &\mathbf{p}_{-N}^* = \mathbf{r}_{-N} + \mathbf{k}_{22}\mathbf{u}_{-N} + \mathbf{k}_{21}\mathbf{u}_N, \\ &\quad \text{because } \mathbf{u}_{-(N+1)} = \mathbf{u}_N \end{aligned} \tag{4.7}$$

$$\mathbf{p}_n^* = \mathbf{p}_n, \qquad n=0,\pm1,\ldots,\pm(N-1) \tag{4.8}$$

$$\begin{aligned} &\mathbf{p}_N^* = \mathbf{r}_N + \mathbf{k}_{12}\mathbf{u}_{-N} + \mathbf{k}_{11}\mathbf{u}_N, \\ &\quad \text{because } \mathbf{u}_{N+1} = \mathbf{u}_{-N} \end{aligned} \tag{4.9}$$

Equation (4.6) can be written in a more compact form as follows

$$\sum_{v=n-1}^{n+1} \mathbf{k}_{n-v}\mathbf{u}_v = \mathbf{p}_n^* \quad n=0,\ \pm1,\ \pm2,\ldots,\ \pm N \tag{4.10}$$

DFT is used to solve equation (4.10). The Fourier transform of vectors $\mathbf{u}_n$, $\mathbf{p}_n^*$ and matrices $\mathbf{k}_n$ are called, respectively, $\tilde{\mathrm{u}}_s$, $\tilde{\mathbf{p}}_s$, and $\tilde{\mathbf{k}}_s$, and they are given by the expressions

$$\tilde{\mathbf{u}}_s = \sum_{n=-N}^{N} \mathbf{u}_n e^{-i\alpha sn} \tag{4.11}$$

$$\tilde{\mathbf{p}}_s^* = \sum_{n=-N}^{N} \mathbf{p}_n^* e^{-i\alpha sn} \tag{4.12}$$

$$\tilde{\mathbf{k}}_s = \sum_{n=-N}^{N} \mathbf{k}_n e^{-i\alpha sn} = \mathbf{k}_0 + \mathbf{k}_{-1}e^{i\alpha s} + \mathbf{k}_1 e^{-i\alpha s} \tag{4.13}$$

$$\begin{aligned} &\text{with } \ i=\sqrt{-1},\ \ \alpha=\frac{2\pi}{2N+1} \ \text{ and} \\ &\quad s=0,\ \pm1,\ \pm2,\ldots,\ \pm N \end{aligned} \tag{4.14}$$

*From a mathematical point of view, due to the ellipticity of the problem, the influence of the boundary conditions represented by equations (2.1) to (2.3) imposed at the beam ends is very small.

When taking DFT to both sides of equation (4.10), the following equations are obtained

$$\sum_{n=-N}^{N}\sum_{v=n-1}^{n+1}\mathbf{k}_{n-v}\mathbf{u}_v e^{-i\alpha sn}=\sum_{n=-N}^{N}\mathbf{p}_n^* e^{-i\alpha sn} \tag{4.15}$$

The first term of equation (4.15) can be rewritten as follows

$$\sum_{n=-N}^{N}\sum_{v=n-1}^{n+1}\mathbf{k}_{n-v}e^{-i\alpha s(n-v)}\mathbf{u}_v e^{i\alpha sv} = \sum_{j=-1}^{1}\mathbf{k}_j e^{-i\alpha sj}\sum_{n=-N}^{N}\mathbf{u}_{n-j}e^{-i\alpha s(n-j)} \tag{4.16}$$

with $j=n-\nu$.

Given that $\mathbf{u}_n$ is a periodic vector with period $2N+1$, it can be written as

$$\sum_{n=-N}^{N}\mathbf{u}_{n-j}e^{-i\alpha s(n-j)}=\sum_{n=-N}^{N}\mathbf{u}_n e^{-i\alpha sn} \tag{4.17}$$

and equation (4.10) results

$$\tilde{\mathbf{k}}_s\tilde{\mathbf{u}}_s=\tilde{\mathbf{p}}_s^* \quad \text{with} \quad s=0,\ \pm1,\ \pm2,\ldots,\ \pm N \tag{4.18}$$

where

$$\tilde{\mathbf{p}}_s^*=\tilde{\mathbf{p}}_s+(\mathbf{r}_{-N}+\mathbf{k}_{22}\mathbf{u}_{-N}+\mathbf{k}_{21}\mathbf{u}_N)e^{is\alpha N} +(\mathbf{r}_N+\mathbf{k}_{12}\mathbf{u}_{-N}+\mathbf{k}_{11}\mathbf{u}_N)e^{-is\alpha N} \tag{4.19}$$

and taking into account the fixed ends of the spans at ends $-N$ and N, equation (4.19) simplifies to

$$\tilde{\mathbf{p}}_s^*=\tilde{\mathbf{p}}_s+\mathbf{r}_N e^{-is\alpha N}+\mathbf{r}_{-N}e^{is\alpha N} \tag{4.20}$$

All loads $\mathbf{p}_n$ acting at internal supports of the structure are 0 except the one acting in span 0-1, and so it is obtained

$$\tilde{\mathbf{p}}_s=\sum_{n=-N}^{N}\mathbf{p}_n e^{-isn\alpha}=\mathbf{p}_0+\mathbf{p}_1 e^{-is\alpha} \tag{4.21}$$

The reader should notice that equation (4.18) can also be obtained directly from equation (4.10) by applying the DTF as a convolution of matrix $\mathbf{k}_n$ and vector $\mathbf{u}_n$.

It should be noted that the inverse of matrix $\tilde{\mathbf{k}}_s$ can be obtained for all values of $s=0, \pm1, \pm2,\ldots, \pm N$, as it has a fixed-end or rigid support at both ends and therefore there do not exist rigid-body movements. Accordingly, the solution in the s-domain is

$$\tilde{\mathbf{u}}_s=\left(\tilde{\mathbf{k}}_s\right)^{-1}\tilde{\mathbf{p}}_s^* \tag{4.22}$$

and taking into account equations (4.20) and (4.21), the following expression is obtained

$$\tilde{\mathbf{u}}_s=\left(\tilde{\mathbf{k}}_s\right)^{-1}[\mathbf{p}_0+\mathbf{p}_1 e^{-is\alpha}+\mathbf{r}_N e^{-is\alpha N}+\mathbf{r}_{-N}e^{is\alpha N}] \tag{4.23}$$

The solution $\mathbf{u}_n$ in the n domain is obtained by applying the inverse to (4.22) and so the following expression is reached

$$\mathbf{u}_n=\frac{1}{2N+1}\sum_{s=-N}^{N}\tilde{\mathbf{u}}_s e^{i\alpha sn}=\frac{1}{2N+1}\sum_{s=-N}^{N}\left(\tilde{\mathbf{k}}_s\right)^{-1}\tilde{\mathbf{p}}_s^* e^{i\alpha sn} \tag{4.24}$$

Equation (4.24) can be expressed in terms of the functions known as cyclic flexibilities $h_{(n1,n2)}$ as follows

$$\mathbf{u}_n=\mathbf{h}_{(N,n)}\mathbf{r}_N+\mathbf{h}_{(-N,n)}\mathbf{r}_{-N}+\mathbf{h}_{(0,n)}\mathbf{p}_0+\mathbf{h}_{(1,n)}\mathbf{p}_1 \tag{4.25}$$

where

$$\mathbf{h}_{(n1,n2)}=\frac{1}{2N+1}\sum_{s=-N}^{N}\left(\tilde{\mathbf{k}}_s^{-1}\right)e^{is\alpha(n2-n1)} \tag{4.26}$$

The unknown reactions $\mathbf{r}_{-N}$ and $\mathbf{r}_N$ are obtained by applying the fix-end conditions at the ends of the structure, i.e. by imposing $\mathbf{r}_{-N}=0$ and $\mathbf{r}_N=0$. Then, at values $n=N$ and $n=-N$, in equation (4.25), the following system of equations is reached

$$\begin{bmatrix}\mathbf{h}_{(N,N)} & \mathbf{h}_{(-N,N)}\\ \mathbf{h}_{(N,-N)} & \mathbf{h}_{(-N,-N)}\end{bmatrix}\begin{bmatrix}\mathbf{r}_N\\ \mathbf{r}_{-N}\end{bmatrix}=-\begin{bmatrix}\mathbf{h}_{(0,N)} & \mathbf{h}_{(1,N)}\\ \mathbf{h}_{(0,-N)} & \mathbf{h}_{(1,-N)}\end{bmatrix}\begin{bmatrix}\mathbf{p}_0\\ \mathbf{p}_1\end{bmatrix} \tag{4.27}$$

and defining the inverse of the first matrix in expression (4.27) as

$$\begin{bmatrix}\bar{\mathbf{h}}_{(N,N)} & \bar{\mathbf{h}}_{(-N,N)}\\ \bar{\mathbf{h}}_{(N,-N)} & \bar{\mathbf{h}}_{(-N,-N)}\end{bmatrix}=\begin{bmatrix}\mathbf{h}_{(N,N)} & \mathbf{h}_{(-N,N)}\\ \mathbf{h}_{(N,-N)} & \mathbf{h}_{(-N,-N)}\end{bmatrix}^{-1} \tag{4.28}$$

the unknown vector of generalized forces (forces and moments) at end nodes of the structure is obtained

$$\begin{bmatrix}\mathbf{r}_N\\ \mathbf{r}_{-N}\end{bmatrix}=-\begin{bmatrix}\bar{\mathbf{h}}_{(N,N)} & \bar{\mathbf{h}}_{(-N,N)}\\ \bar{\mathbf{h}}_{(N,-N)} & \bar{\mathbf{h}}_{(-N,-N)}\end{bmatrix}\begin{bmatrix}\mathbf{h}_{(0,N)} & \mathbf{h}_{(1,N)}\\ \mathbf{h}_{(0,-N)} & \mathbf{h}_{(1,-N)}\end{bmatrix}\begin{bmatrix}\mathbf{p}_0\\ \mathbf{p}_1\end{bmatrix} \tag{4.29}$$

Once this vector of generalized forces, $\mathbf{r}_N$ and $\mathbf{r}_{-N}$, is known, the corresponding vector of generalized displacements (i.e. displacement and rotation) at each node n is obtained from equation (4.25). Finally, for each span n, joining supports $n-1$ and n, forces and reactions at its end nodes can be computed by applying formulae (3.3).

In same cases, it is not sufficient to know the generalized displacements in all supports n, with $n=-N$, $-(N-1),\ldots, N-1, N$. It can then be of interest to obtain the elastic of a beam n along its span between its supports $n-1$ and n, i.e. the vector function $\mathbf{u}_{n\xi}=(u)_n(\xi)$.

In the following, the deflection curve of the structure will be derived. The generalized displacement vector $\mathbf{u}_{n\xi}$, at section ξ of the beam n, contains the deflection $\bar{v}_{n\xi}$ and the rotation $\bar{\theta}_{n\xi}$, produced at section ξ of beam n distant ξ of support $n-1$. It is assumed the general case where the load $\bar{P}$, applied at section $\bar{a}$ of the span is acting on beam n. The case of a load acting on a support is easily introduced by assuming $\bar{a}=0$. The beam n deflexion curve is obtained by applying the following expression

$$\mathbf{u}_{\xi n}=\begin{bmatrix}\bar{v}_{n\xi}\\ \bar{\theta}_{n\xi}\end{bmatrix}=\begin{bmatrix}\mathbf{N}_{11}(\xi) & \mathbf{N}_{12}(\xi)\\ \mathbf{N}_{21}(\xi) & \mathbf{N}_{22}(\xi)\end{bmatrix}\begin{bmatrix}\mathbf{u}_{n-1}\\ \mathbf{u}_n\end{bmatrix}+\mathbf{u}^0_{\xi n} \tag{4.30}$$

where $\mathbf{u}^0_{\xi n}$ are the generalized displacements due to the acting load $\bar{P}$ on the beam n span only

$$\mathbf{N}_{11}(\xi)=[N_1(\xi)\ \ N_2(\xi)],\quad \mathbf{N}_{12}(\xi)=[N_3(\xi)\ \ N_4(\xi)] \tag{4.31}$$

$$\mathbf{N}_{21}(\xi)=[N_1'(\xi)\ \ N_2'(\xi)],\quad \mathbf{N}_{22}(\xi)=[N_3'(\xi)\ \ N_4'(\xi)] \tag{4.32}$$

$$\mathbf{u}^0_{\xi n}=\begin{bmatrix}\bar{v}^0_{\xi n}\\ \bar{\theta}^0_{\xi n}\end{bmatrix} \tag{4.33}$$

and the functions $N_i(\xi)$ are interpolation functions known as Hermite polynomials

$$N_1(\xi)=1-3\xi^2+2\xi^3,\quad N_2(\xi)=\xi-2\xi^2+\xi^3 \tag{4.34}$$

$$N_3(\xi)=3\xi^2-2\xi^3,\quad N_4(\xi)=-\xi^2+2\xi^3 \tag{4.35}$$

$$N_j'=\frac{dN_j(\xi)}{\mathrm{d}\xi},\ (j=1,2,3,4) \tag{4.36}$$

$$\begin{aligned}\bar{v}^0_\xi&=\frac{1}{6}\bar{b}\xi(1-\bar{b}^2-\xi^2)\bar{P}\ (0\le\xi\le\bar{a}),\\ \bar{v}^0_\xi&=\frac{1}{6}\bar{a}(1-\xi)[1-\bar{a}^2-(1-\xi)^2]\bar{P}\ (\bar{a}\le\xi\le 1)\end{aligned} \tag{4.37}$$

$$\begin{aligned}\bar{\theta}^0_\xi&=\frac{1}{6}\bar{b}(1-\bar{b}^2-3\xi^2)\bar{P}\ (0\le\xi\le\bar{a}),\\ \bar{\theta}^0_\xi&=-\frac{1}{6}\bar{a}[1-\bar{a}^2-3(1-\xi)^2]\bar{P}\ (\bar{a}\le\xi\le 1)\end{aligned} \tag{4.38}$$

Reactions over the sleepers can be easily obtained using the well-known linear relationship between the force and displacement given by

$$R=k\,u \tag{4.39}$$

5 COMPUTER PROGRAM IN MatLab

Based on the theory presented in Section 4, a program in MatLab has been written. It can be observed the simplicity of the program that is composed by a relative small number of statements. This program allows to compute the generalized displacements and forces produced in the rail track. The complete code can be downloaded from the web site: http://www.samartin.es/software/matlab/DFTRailwayTrack/.

For ease of exposition, the program follows closely the theoretical steps of Section 4, and hence, the DFT subroutines available in MatLab have not been used. Using Matlab for the DFT with FFT implementation important additional computational time savings could be reached.**

The results shown in this article, and some more, can be obtained executing program0.m, program1.m, and program2.m. There is also program3.m to plot the shape functions used to obtain intermediate results between two consecutive nodes.

6 APPLICATION EXAMPLES

The following data have been used to model the track: Sleeper span $L=0.60$ m. Rail UIC-60 type with a flexural stiffness of $EI=6,426\times10^6$ Nm^2, a cross-section area of 7687 mm^2, ground spring constant $k=$ 31,581,740.98 N/m, and load of one wheel over a rail $P=(18\cdot10^3/2)9.8=88{,}200$ N. The calculations have been done with the dimensionless parameters described in Section 3. The sensitivity of the load location at the first beam element a and the support spring constant k has been studied.

Table 2 presents the relative vertical displacements of central sleepers, $\bar{v}_n$, for $n=\pm7,\pm6,\ldots,\pm1$, when the wheel load is at node 0. These results are compared with the traditional methods used in railway technology Lorente (L) [**15**] and Zimmermann–Timoshenko (ZT) [**19**, **20**]. There is a great similarity between the three of them. However, the L method is much closer to the new proposed method. The obtained results can even be considered to be quite accurate for a small value of N.

Nevertheless, if the usual methods L and ZT are compared with the new one, the absolute error $\Delta_L=\bar{v}_{nL}-\bar{v}_n$ as well as the relative one $\varepsilon_L=\frac{\bar{v}n-\bar{v}_{nL}}{\bar{v}_n}$ of the L method are smaller than the corresponding error values Δ_{ZT} and ε_{ZT} of the ZT.

** *These subroutines are based on the Fast Fourier transform (FFT). This algorithm developed in reference [**18**] reduces the computation time respect to the direct DFT as the ratio* $\log_2(N)/N$, *where* N *is the number of points.*

With these values, the reactions in the sleepers have been determined when $P = 88.20$ kN load applied is over the central sleeper. Table 3 gives the value of these reactions and the percentage of the total load transmitted to the ground by each support.

A sensitivity analysis of the main dimensionless parameters is also carried out and it is shown in the following figures. This analysis could be useful for an initial design taking into account the vertical railway stiffness $\bar{k}$.

The vertical displacement of node 0 $\bar{v}_0$, for different load $\bar{P}$ positions, between sleepers 0 and 1 ($\bar{a}$), as a function of the vertical railway stiffness $\bar{k}$, has been calculated. Figure 3(a) shows the 3D representation of this displacement. Figure 3(b) to (d) shows 2D views of this 3D representation by equally spaced planes perpendicular to each of the axes.

Figure 4 shows the deformed shape of the railway track extended to seven elements at each side of element 1, when the load is applied at the following dimensionless locations $\bar{a} = 0.00$, 0.25, 0.50, 0.75, and 1.00 of this element.

Table 3 shows vertical displacements, reactions, and relative reactions of the sleepers due to the applied loads on the rail. These results are obtained when the load is located in the middle of the span 0-1 and on node 0.

When the load is in the middle of the span 0-1, the maximum deflection is 1.006,675 mm compared to the deflection of 0.999,849 mm on the sleeper when the wheel is over it. That means that the wheel does not travel over a perfectly straight horizontal rail, but it travels over a periodic curve with can be approximated by a sinusoid of 0.60 m wavelength and a very small amplitude of $1.006{,}675 - 0.999{,}849 = 0.006{,}826{,}40$ mm. This causes two phenomena: (1) creating the well-known sleeper frequency in the vertical acceleration of the axle box and (2) causing the unsprung masses (axle and wheels) and sprung masses (truck and passenger box) to be excited by this sinusoidal movement. This phenomenon causes high increments of the vertical axle accelerations and the corresponding dynamic loads can damage seriously the ballast and the track. The

Table 2 Vertical displacements with the proposed method $\bar{v}_n$, compared to Lorente (L) $\bar{v}_{nU}$ [**15**] and Zimmermann–Timoshenko (ZT) $\bar{v}_{nZT}$ [**19, 20**]

Node n (-)	Different calculation methods						
	Proposed	Lorente			Zimmermann–Timoshenko		
	$\bar{v}_n$ (mm)	$\bar{v}_{nL}$ (mm)	Δ_L (mm)	ε_L ($\frac{\%}{1000}$)	$\bar{v}_{nZT}$ (mm)	Δ_{ZT} (mm)	ε_{ZT} (%)
−7	−4.26964e−3	−4.27000e−3	−3.59e−10	−8.4274	−4.19200e−3	7.76e−8	1.8184
−6	−1.77637e−2	−1.77640e−2	−3.30e−10	−1.8577	−1.76240e−2	1.39e−7	0.7862
−5	−3.69211e−2	−3.69210e−2	5.64e−11	0.1528	−3.67950e−2	1.26e−7	0.3414
−4	−3.94121e−2	−3.94120e−2	1.33e−10	0.3385	−3.95040e−2	−9.18e−8	−0.2330
−3	3.33383e−2	3.33380e−2	−3.47e−10	1.0412	3.27690e−2	−5.69e−7	1.7077
−2	2.68432e−1	2.68432e−1	−3.85e−11	0.0143	2.67376e−1	−1.05e−6	0.3934
−1	6.88856e−1	6.88856e−1	−4.23e−10	0.0614	6.87929e−1	−9.27e−7	0.1346
0	9.99849e−1	9.99849e−1	2.38e−12	−0.0002	9.99915e−1	6.60e−8	−0.0066
1	6.88856e−1	6.88856e−1	−4.23e−10	0.0614	6.87929e−1	−9.27e−7	0.1346
2	2.68432e−1	2.68432e−1	−3.85e−11	0.0143	2.67376e−1	−1.05e−6	0.3934
3	3.33383e−2	3.33380e−2	−3.47e−10	1.0412	3.27690e−2	−5.69e−7	1.7077
4	−3.94121e−2	−3.94120e−2	1.33e−10	0.3385	−3.95040e−2	−9.18e−8	−0.2330
5	−3.69211e−2	−3.69210e−2	5.64e−11	0.1528	−3.67950e−2	1.26e−7	0.3414
6	−1.77637e−2	−1.77640e−2	−3.30e−10	−1.8577	−1.76240e−2	1.39e−7	0.7862
7	−4.26964e−3	−4.27000e−3	−3.59e−10	−8.4274	−4.19200e−3	7.76e−8	1.8184

Table 3 Displacements, reactions, and relative reactions for $\bar{a} = 0.5$ and $\bar{a} = 0.0$

Node	Load in middle of the span			Load on the sleeper		
	Displacement (mm)	Reaction (kN)	Reaction./load (%)	Displacement (mm)	Reaction (kN)	Reaction./load (%)
0	−0.90227 5	−28.49541 1	32.30772	−0.99984 9	−31.57697 2	35.80155
1	−0.90227 5	−28.49541 1	32.30772	−0.68885 6	−21.75528 5	24.66585
2	−0.46331 5	−14.63228 8	16.58989	−0.26843 2	−8.47755 1	9.61173
3	−0.12581 9	−3.97357 0	4.50518	−0.03333 8	−1.05288 3	1.19374
4	0.01781 9	0.56274 8	−0.63803	0.03941 2	1.24470 3	−1.41122
5	0.04306 7	1.36012 2	−1.54208	0.03692 1	1.16603 1	−1.32203
6	0.02742 5	0.86614 0	−0.98201	0.01776 4	0.56100 7	−0.63606
7	0.00075 6	0.02388 8	−0.02708	0.00427 0	0.13484 2	−0.15288

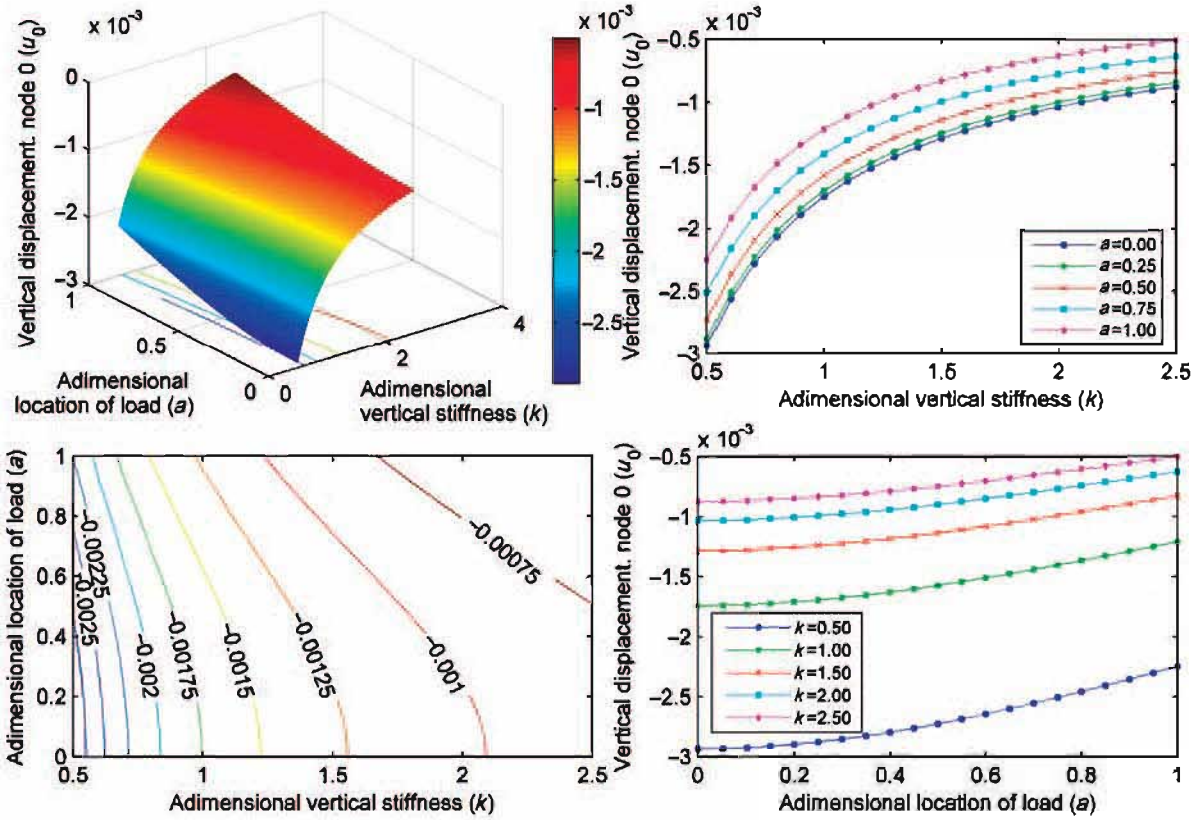

Fig. 3 Vertical displacement $\bar{v}_0$ as function of $\bar{a}$ and $\bar{k}$

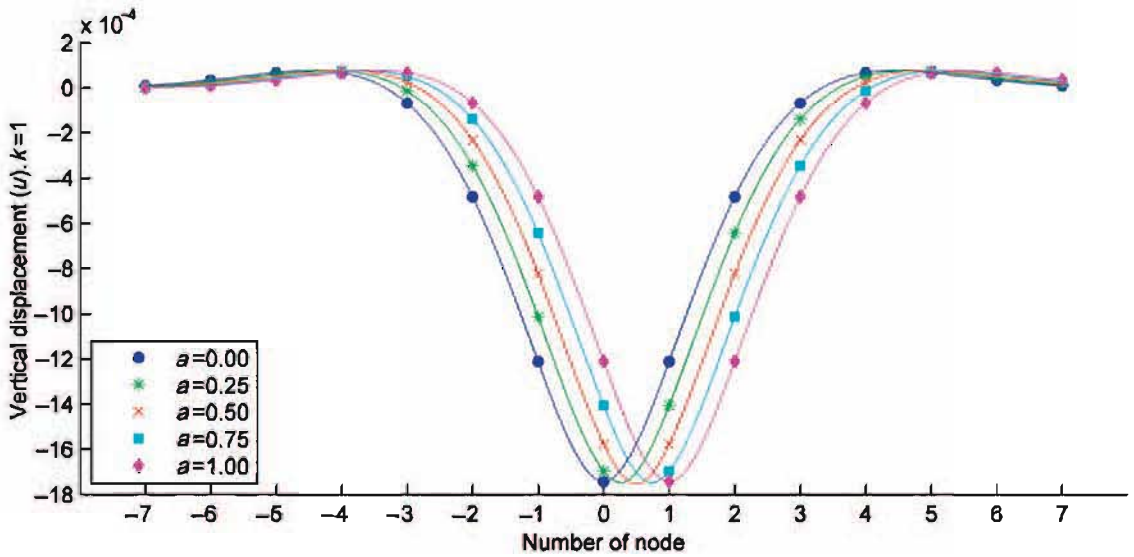

Fig. 4 Deformed shape of the rail with the load $\bar{P} = 1.0$ at section ā of beam element 1

phenomenon has also been used to explain the occurrence of derailed axles in long trains.

When the rail is of type UIC-54 with a flexural rigidity of $EI = 4.47401 \times 10^6$ Nm^2 instead of UIC-60 and the same remaining data, the following results could be reached: 1.104,369 − 1.093,291 = 0.011,078 mm, i.e. an amplitude 62.3 per cent larger than the former one.

A comparison of the computing time between standard structural matrix analysis represented by the commercial software ANSYS and the MATLAB scripts has been carried out in the same computer (Intel Core 2 Duo T9600 at 2.80 GHz with 8 GB RAM). A hundred simulations have been performed with 201 and 2001 rail elements, each between consecutive sleepers, to

obtain the mean, standard deviation, and minimum and maximum time values, as shown in Table 4. The ANSYS graphical and text outputs have been deactivated. Time is measured from data input until displacements are obtained. The extra time to print out results is not considered in either case. From these results, it can be concluded that ANSYS requires nearly 20 times more to carry out the same analysis. A further improvement in computational time can be achieved with the use of the FFT instead of a DFT.

It should be pointed out that the input data of the proposed program require only seven parameters. This makes it a simple and friendly program to use. This is a clear advantage compared to any general structural analysis software.

In the last example, it is shown the capabilities of the proposed method of analysis to handle different groups of spatially periodic structures. In this example, a very long non-periodical track is modelled as a set of several substructures that are easily defined. The assembly of these substructures follows the usual procedures of matrix structural analysis.

Figure 5 shows an example where the rail track is formed by three periodic substructures joined together. The first and third one, with 50 elements each, have a span length between sleepers of 0.60 m, while the second one, with the same number of elements has a span length of 1.20 m. The sleeper span may be varied to spread the energy of vibration. The vertical stiffness of the track in the first and second substructures has been taken as $k=3.16e7$ N/m, while in the third structure, a value of $k=5.66e7$ N/m has been considered. This accounts for possible changes in the soil rigidity, as it can be to enter and structure or to consider different ballast embankments. Also, material (Young's modulus, $E=2.1e11$ N/m^2) and mechanical (inertia $I=3055e-8$ m^4) properties of the rail may change between substructures, but they are not considered in the following example. Loads of 88200 N have been placed at the middle of each substructure.

7 CONCLUSIONS

In this article, a method of analysis of a railroad track is presented. The method is based on a general treatment of analysis of spatially periodic structures, i.e. structures composed by a repetitive simpler structure. By applying a DFT, the computational effort is substantially reduced, as the total number of resulting stiffness equilibrium equations $q(2N+1)$ to be solved is modified to a set of $2N+1$ uncoupled systems of q equations each, particularly in the analysis of railways track roads structures.

Table 4 Comparison of computational times between the proposed method and ANSYS

	MATLAB				ANSYS			
Number of elements	Mean (s)	σ (s)	Min (s)	Max (s)	Mean (s)	σ (s)	Min (s)	Max (s)
201	0.0531	0.0021	0.0516	0.0720	0.9777	0.0707	0.8586	1.3104
2001	0.5126	0.0030	0.5055	0.5198	9.1742	2.3200	7.5816	14.1649

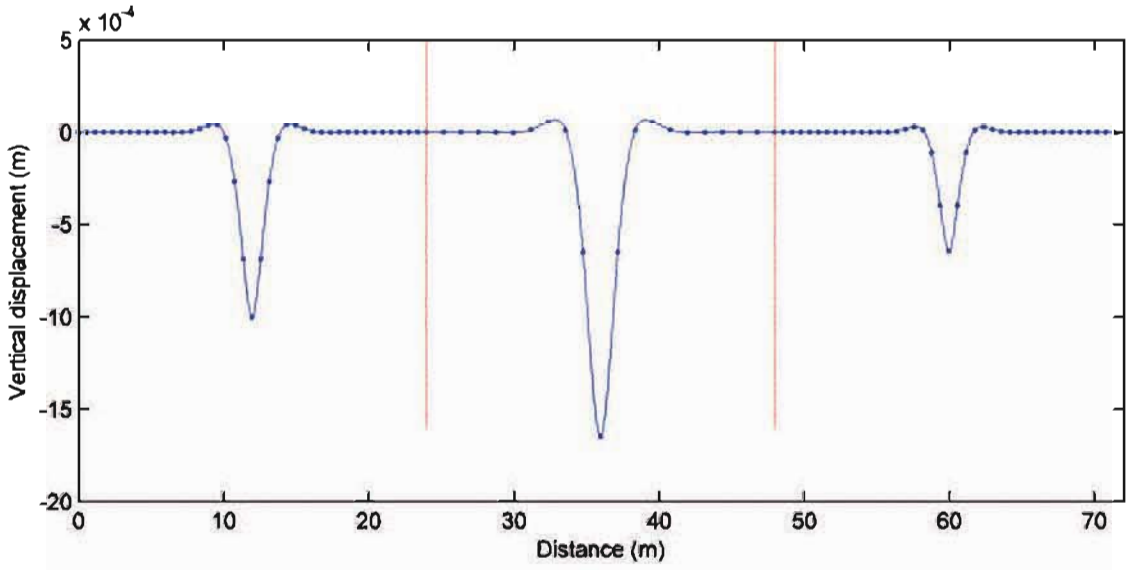

Fig. 5 Deformed shape of the rail formed by three different substructures joined together

The results obtained by the proposed method are exact in the context of linear elastic analysis of structures, that means, they coincide with the ones found by other alternative methods, such as Lorente de Nó or matrix methods of structural analysis (transfer matrix, flexibility and stiffness methods), although the latter are obtained with more computational effort. The results found with the proposed method totally coincide with those reached by the Lorente de Nó method. Additionally, if the ballast coefficient is properly chosen, they are also coincident with those reached by the Zimmermann–Timoshenko model. The difficulty with the Zimmermann–Timoshenko model is that the engineer using it has to guess not only the ballast coefficient but also a certain width b of the model in which this coefficient would apply.

Another advantage of the proposed method is that it avoids the difficulty found in the Zimmermann–Timoshenko model of estimating the value of the ballast coefficient or modulus C. Nowadays, there is no practical and useful method for its evaluation, whereas the measure of the rail deflection is a simple and common task.

The simplicity of the proposed method is shown in its formulation that can essentially be reduced to equations (4.25) and (4.26), and to the solution of the system (4.27) in order to obtain the unknown reactions $\mathbf{r}_{-N}$ and $\mathbf{r}_N$ at end nodes −N and N, of the whole structure.

Finally, it should be noted that this approach of analysis and programming can be easily extended to other types of periodic structures, by changing the expressions of the stiffness matrices $\mathbf{k}_{ij}$ $(i, j = 1, 2)$ and the dimensions of the new vectors and matrices involved, i.e. the q degrees of freedom of the common nodes connecting adjacent elements. Details can be seen in Samartín [**1**].

FUNDING

This research is partially financed by the Spanish Ministry of Science and Innovation (project reference P8/08) within the National Plan for Scientific Research, Development and Technological Innovation 2008-2011.

REFERENCES

1 **Samartín, A.** Analysis of spatially periodic structures. Application to shell and spatial structures. In Proceedings of I.A.S.S. Symposium on *Innovative applications of shell and spatial structures.* Bangalore (India), vol. III, 1988, pp. 205–221 (Oxford and IBH Publishing Ltd).

2 **Hussey, M. J. L.** General theory of cyclically symmetric frames. *ASCE. J. Struct. Div.*, 1967, **93**(4), 360–368.

3 **Thomas, D. L.** Dynamics of rotationally periodic structures. *Int. J. Numer. Methods Eng.*, 1979, **14**, 81–102.

4 **Cai, C. W., Cheung, Y. K.,** and **Chan, H. C.** Dynamic response of infinite continuous beams subjected to a moving force-an exact method. *J. Sound Vib.*, 1988, **123**(63), 461–472.

5 **Cheung, Y. K., Chan, H. C.,** and **Cai, C. W.** Exact method for static analysis of periodic structures. *ASCE. J. Eng. Mech.*, 1989, **115**(2), 415–434.

6 **Chebli, H., Othman, R.,** and **Clouteau, D.** Response of periodic structures due to moving loads. *Mechanique*, 2006, **334**, 347–352.

7 **Moore, G.** Floquet theory as a computational tool. *SIAM J. Numer. Anal.*, 2005, **42**(6), 2522–2568.

8 **Amann, H.** *Ordinary differential equations*, 1990 (Walter de Gruyter, Berlin).

9 **Hale, J.** *Ordinary differential equations*, 1969 (Wiley-Interscience, New York).

10 **Esveld, C.** *Modern railway track*, 2nd edition, 2001 (MRT Productions, Zaltbommel).

11 **Melis, M.** *Apuntes de introducción a la dinámica vertical de la via y a las señales digitales en ferrocarriles. Con 151 programas en Matlab, Simulink, Visual C++, Visual Basic y Excel*, 2008 (Escuela Técnica Superior de Ingenieros de Caminos Canales y Puertos, Universidad Politécnica de Madrid, Madrid).

12 **Samartín, A.** *Resistencia de Materiales*, 1995 (Colegio de Ingenieros de Caminos, Canales y Puertos, Madrid).

13 **Unold, G.** *Statik für den Eisen und Maschinenbau.*, 1925 (Springer Verlag, Berlin, Germany).

14 **Dischinger, F.** Der Durchlaufende Träger und Rahmen auf elasticher senkbaren Stützen. *Der Bauengenieur*, 1942, **9/10**, 15–27.

15 **Lorente de Nó.** Geotecnia y Cimientos. vol. 3, chapter 1.1.7, *Viga continua sobre apoyos elásticos*, 1980, pp. 27–50 (Editorial Rueda, Madrid).

16 **Livesley, R. K.** *Matrix Methods of structural analysis*, 1975 (Pergamon Press, Oxford).

17 **Karpov, E. G., Stephen, N. G.,** and **Dorofeev, D. L.** On static analysis of finite repetitive structures by discrete Fourier transform. *Int. J. Solids Struct.*, 2002, **39**, 4291–4310.

18 **Cooley, J. W.** and **Tukey, J. W.** An algorithm for machine calculation of complex Fourier series. *Math. Comput.*, 1965, **19**, 297–301.

19 **Zimmermann, H.** *Die Berechnung des Eisenbahn-Oberbaues.*, 1930 (Springer Verlag, Berlin).

20 **Timoshenko, S. P.** *History of strength of materials.*, 1953 (McGraw Hill, New York).